IGNITED RELEASES OF LIQUID HYDROGEN: SAFETY CONSIDERATIONS OF THERMAL AND OVERPRESSURE EFFECTS

Hall, J.E.[1], Hooker, P.[2] and Willoughby, D.[3]

Major Hazards Unit, Health and Safety Laboratory, Harpur Hill, Buxton, SK179JN, England,
[1]jonathan.hall@hsl.gsi.gov.uk
[2]philip.hooker@hsl.gsi.gov.uk
[3]deborah.willoughby@hsl.gsi.gov.uk

ABSTRACT

If the 'Hydrogen Economy' is to progress, more hydrogen fuelling stations are required. In the short term and in the absence of a hydrogen distribution network, these fuelling stations will have to be supplied by liquid hydrogen (LH2) road tankers. Such a development will increase the number of tanker offloading operations significantly and these may need to be performed in close proximity to the general public.

LH2 was first investigated experimentally [1] as large-scale spills of LH2 at a rate of 60 litres per minute. Measurements were made on un-ignited releases which included the concentration of hydrogen in air, thermal gradients in the concrete substrate, liquid pool formation and temperatures within the pool. Computational modelling on the un-ignited spills was also performed [2]. The experimental work on ignited releases of LH2 detailed in this paper is a continuation of the work performed by Royle and Willoughby [1].

The experimental findings presented are split into three phenomena; jet-fires in high and low wind conditions, 'burn-back' of ignited clouds and secondary explosions post 'burn-back'. The aim of this work was to determine the hazards and severity of a realistic ignited spill of LH2 focussing on; flammability limits of an LH2 vapour cloud, flame speeds through an LH2 vapour cloud and subsequent radiative heat levels after ignition. An attempt was made to estimate the magnitude of an explosion that occurred during one of the releases. The results of these experiments will inform the wider hydrogen community and contribute to the development of more robust modelling tools. The resulting data were used to propose safety distances for LH2 offloading facilities which will help to update and develop guidance for codes and standards.

1. INTRODUCTION

The 'Hydrogen Economy' is gathering pace internationally and now in the UK. Over the last year a number of vehicle related demonstration projects have appeared, linked to the 2012 Olympics. Whilst in the long term, the key to the development of a hydrogen economy is a full infrastructure to support it, a short bridging option for hydrogen refuelling stations particularly, is the bulk storage and transport of cryogenic hydrogen, referred to in industry as LH2. LH2 storage and transport are the most efficient and cost effective means of rapidly implementing hydrogen distribution. This will result in moderately large inventory, local storage of LH2 e.g. the Olympic refuelling station. Although cryogenic liquid storage has been used safely for many years in secure and regulated industrial sites, its use in relatively congested highly populated urban areas presents a new set of problems in relation to security, safety and associated planning. There is previous work undertaken by NASA on LH2 relating to its spill behaviour [3], but this was performed in a low humidity desert environment. In addition, it did not cover issues around leakage and combustion behaviour thoroughly as these problems were managed by the controls possible in an isolated specialist facility on the large remote sites used.

Research is therefore needed to identify and address issues relating to bulk LH2 storage facilities associated with hydrogen refuelling stations located in urban environments so that further guidance on their safe management can be developed.

Issues in particular relating to LH2 include: flame speed, ignition behaviour as a cool/dense vapour and the complications of this associated with layering effects, LH2's low boiling point and associated ability to condense out and even solidify oxygen from air to produce a potentially hypergolic mixture of LH2 and liquid or solid oxygen.

Table 1. Properties of Hydrogen and the main constituents of air

	Hydrogen	Nitrogen	Oxygen
Liquid density (kg/m^3)	70	807	1141
Gas density at boiling point (kg/m^3)	1.3	4.6	4.5
Boiling point (K)	20.28	77.36	90.19
Freezing point (K)	14.01	63.15	50.5

1.1. Un-ignited Releases

During 2009-2011 Royle and Willoughby performed experiments on large-scale un-ignited releases of liquid hydrogen [1] with the aim of determining the range of hazards from a realistic release of LH2. A number of areas of spill behaviour were investigated:

- Hydrogen dispersion from un-ignited spills;
- On ground liquid pool formation;
- Spills into free air;
- Pool formation with respect to storage conditions.

The work involved releasing LH2 at fixed conditions of 1 barg in the tanker through 20 m of 1" n.b. hose, which gave a rate of 60 litres per minute for differing durations. The release height and orientation were varied and the sensor positions were changed. During testing experimental measurements were made on:

- Hydrogen concentration – temperature measurements were taken at 30 positions in air at a range of heights and distances from the release point in line and downwind of the wind;
- Pool extent – 24 thermocouples in line with the release and visual records;
- Thermal gradient in the ground – three thermocouples were embedded into the concrete substrate at depths of 10, 20 and 30 mm.

An example of a horizontal release along the ground can be seen in Fig. 1. The visible cloud in Fig. 1, observed two minutes into the release, extends approximately 10 m across and 8 m high.

Figure 1. Visible cloud approximately 8m high

The conclusions from this work were as follows:

- The release of LH2 in contact with a concrete surface can give rise to pooling of liquid once the substrate is sufficiently cooled;
- Release of LH2 in close proximity to a concrete surface can result in sub-cooling due to vaporisation;
- The release of LH2 at a rate consistent with the failure of a 1 inch transfer line produces a flammable mixture at least nine metres downwind of the release point;
- The release of hydrogen in contact with a concrete surface produces a solid deposit of oxygen and nitrogen once the substrate is sufficiently cooled.

1.2. Aims of Investigation into Ignited Releases

This series of experiments followed on from the un-ignited experimental results (summarised above) to establish the severity of an ignition from a release of LH2 with comparable spill rates, consistent with a transfer hose operation.

A number of distinct areas relating to an ignition were investigated:

- Flammable extent of a vapour cloud;
- Flame speeds through a vapour cloud;
- Radiative heat levels generated during ignition.

2. EXPERIMENTAL SET UP

The facility was situated at the Frith Valley site at the Health and Safety Laboratory in Buxton (Fig. 2 and 3). A process and instrumentation diagram (P&ID) of the release facility is shown in Fig. 4.

Figure 2. LH2 tanker, vacuum line and vent stack

Figure 3. Release point with metal shield

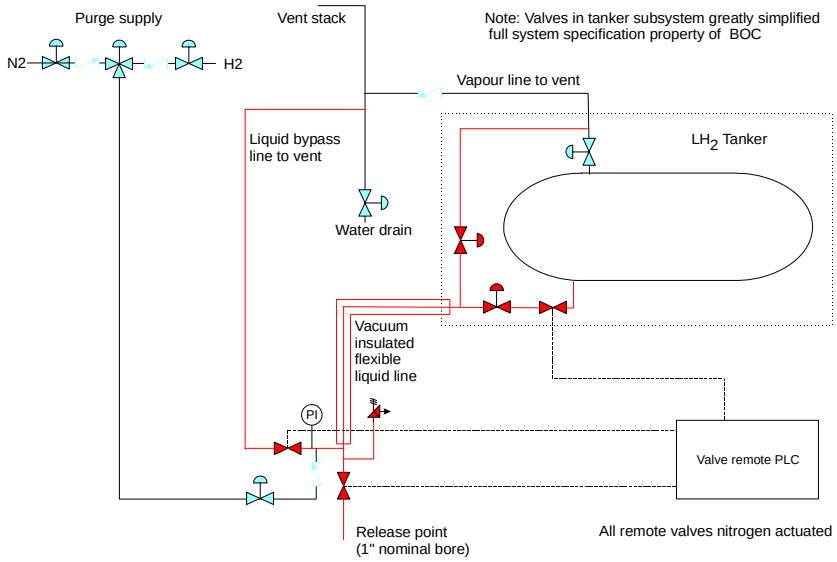

Figure 4. P&ID of the release facility

2.1. Release Facility

The LH2 release system comprised the 2.5 tonne capacity LH2 tanker, 20 metres of 1" n.b. vacuum insulated hose, a release valve station with bypass purge and release valves, a LH2 bypass hose and a 6 m high vent stack to vent excess hydrogen.

On receipt of delivery, the hydrogen within the tanker was normally at around 4 bar pressure and as such it was super-heated relative to its atmospheric boiling point of 20 K. In order to achieve a liquid spill of the contents at atmospheric pressure without excessive flash vaporisation, the tanker was first depressurised to atmospheric pressure by venting hydrogen from the vapour space above the liquid, thereby cooling the remaining LH2 within the tanker to its atmospheric boiling point. Some LH2 was then allowed to flow into the hydrogen/air heat exchanger where it vaporised. This hydrogen vapour was fed to the top of the tanker in order to re-pressurise the LH2 such that it would flow out of the tanker at a nominal flow rate (60 l/min) when the release valve was opened.

Additionally for these ignited trials, a metal shield 1.26 m x 1.6 m was fitted to protect the release point from fire or overpressure damage (Fig. 3). A 5 m radius was also drawn to aid in the location of any interesting phenomena and flame speed measurement.

2.2. Instrumentation

During the tests the following measurements were made:

- Flammable extent and flame speed: two standard definition video cameras at 25 fps, a high speed camera at 500 fps, a modified stills camera for infrared (IR) light only and an FLIR© video camera at 25 fps were used to determine flame speed and flammable extent visually;
- Radiative heat: six fast response (50 ms) ellipsoidal radiometers were used to measure radiative heat, with a range of 110 kW/m^2 with a 160° field of view. The sensors were mounted on poles at a height of 1.8 m and were located downwind and parallel with the release point, separated by 2 m intervals;
- Meteorological measurement: the wind speed and direction were recorded at close proximity to the release point using an ultra-sonic anemometer. Air temperature, relative humidity, wind speed and direction were also measured at the edge of the release pad by a Vector Instruments© weather station.

2.3. Ignition System

To ignite the hydrogen vapour cloud 1kJ Sobbe chemical igniters were used at four positions on the test pad. The optimum positions for the igniters were established using concentration data taken from previous un-ignited tests. The igniters were mounted on stands at a height of 1.5 m facing towards the release point.

3. RESULTS

Fourteen tests were performed in total, of which four were non-ignitions. The reason for the non-ignitions is not clear; it may be that the gas cloud was under or over-rich in hydrogen at the point that the igniters were fired due to differing dispersion and wind effects, or a quenching effect was created by the water vapour created by the cold hydrogen cloud.

Of the tests in which an ignition did occur, typically there was a soft report followed by a low rumble and then a gentle jet flame as the hydrogen issuing from the release pipe burned. During the test programme the ignition delay was varied between ~60 and ~320 seconds. The longer tests allowed for a larger build-up of flammable cloud and also reproduced the liquid/solid pooling phenomena first seen during un-ignited releases of LH2 [1]. The extent of the flammable cloud appeared to be congruent with the visible extent of the water vapour cloud created by the very cold hydrogen cloud when IR footage was compared with visible footage. The flame speeds were measured for each test from the high-speed video and found to develop from 25 m/s up to 50 m/s with increasing release duration. Fig. 5 and 6 show a visible light camera still and an IR still respectively of the ignited hydrogen cloud during different tests.

Figure 5. Camera still of ignited hydrogen cloud

Figure 6. IR still of ignited hydrogen cloud

On one occasion the burning characteristics changed as the cloud was ignited; it burnt back to source creating a jet-fire and then a secondary explosion appeared to emanate from the liquid/solid pool location. The separate phases of the burning cloud are highlighted in the radiometer plot from the test, shown Fig. 7. The first peak on the plot represents the initial deflagration of the cloud back to the release point or ‘burn-back’; the second larger peak represents the secondary explosion and the longer radiative phase after represents the resulting jet-fire. The varying plot levels correspond to the six radiometers located at increasing distances from the release point.

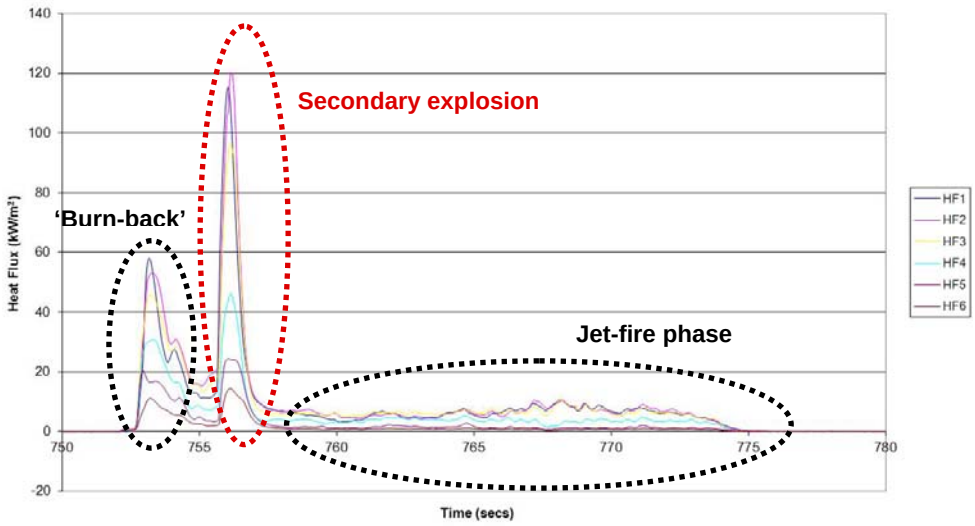

Figure 7. Radiometer readings from ignited release exhibiting a secondary explosion (Test C)

3.1. Secondary Explosion

The secondary explosion occurred close to the release point after the LH2 had been released at ground level, during windy conditions, for 258 seconds without significant pre-cooling of the concrete. The explosion occurred after the hydrogen cloud had been ignited, burned back to the release point and then burned steadily for 3.6 seconds. From IR video footage, the explosion was estimated to be of a hemispherical profile and approximately 8 m in diameter, emanating 2.5 m from the release point, corresponding with the location of the solid/liquid pool seen prior to ignition.

Several attempts were made to reproduce this phenomenon without success, although the conditions on subsequent occasions were far less windy, with the wind in the opposite direction. It is possible that oxygen enrichment of the condensed air may have occurred due to oxygen's higher boiling temperature (90.19 K) than nitrogen (77.36 K), an effect that may have been more likely during the windy conditions. It is postulated that the explosion was either a gas phase explosion resulting from a sudden release of oxygen from the solid due to a rapid phase change, or even a rapid reaction within the condensed slurry of solidified air and LH2 if the oxygen concentration were high enough [3]. Unfortunately, at the time of the explosion no pressure measurements were being made. Therefore, it was necessary to estimate the "size" of the explosion by other means.

3.2. Blast Modelling

As no over-pressure measurements were made at the time of secondary explosion, an estimate of the TNT equivalent energy (derived by one of two methods, below) was used to determine the magnitude of the explosion over-pressure. A blast-modelling program was then used to process this TNT equivalent to provide a visual representation of the pressure.

3.2.1. Method 1 - Pressure effects

The explosion failed to break the Perspex windows in the small cabin approximately 20 m from the centre of the explosion. Knowing the material composition of the window (Perspex) and the distance from the epicentre, it is possible to input this data into the Hazl model to estimate the TNT equivalent required to break a window of comparable dimensions. The modelling program used does not contain data for Perspex specifically and cannot be readily altered to include it; however, an assessment of the upper limit can be made for Polycarbonate, which is stronger than Perspex.

The program calculated that the minimum required TNT equivalent was 4.01 kg for Polycarbonate. From this estimate a TNT equivalent of < 4 kg can be assumed for the explosion. If the hydrogen were to act like a condensed phase explosive i.e. all of the hydrogen is used to generate the blast wave, then this would equate to < 150 g of hydrogen yielding approximately 18 MJ.

3.2.2. Method 2 - Radiative fraction

Another method of estimating the size of the secondary explosion is to use the radiometer data and relate it to the radiative fraction. The fraction of potential heat release that is emitted in the form of radiation is referred to as the radiative fraction, χ, and is defined in Equation 1.

$$Q_r = \chi M \Delta H_c \quad (1)$$

where Q_r - heat radiated, kW; χ - radiative fraction (between 0 and 1); M - mass rate of fuel combustion, kg/s; ΔH_c - heat of combustion of the fuel, kW/kg.

The radiative fraction depends upon the fuel type and whether contaminants are present within the burning cloud. Hydrogen flames typically radiate less than flames from the combustion of hydrocarbon gases. The radiative fraction was estimated for the steady burning periods of the LH2 release experiments, that is after the initial cloud had burned back and the hydrogen was being consumed as it was released and evaporated.

It is common to approximate the radiative fraction of a flame based on radiometer readings taken at a significant distance from the flame such that an inverse square law can be reasonably applied. However, in this case the flame was elongated along the line of the radiometers and was generally close to the ground. It can be seen that the readings of the first three radiometers are very similar to each other (Fig. 7). This would be expected from the flame shape observed on the video recordings. For this reason, a semi-cylindrical radiating heat source was assumed for the purposes of estimating the radiative fraction and the total radiated heat estimated using Equation 2.

$$Q_r = (1 + \alpha)\frac{\pi d L q}{2} \quad (2)$$

where Q_r - heat radiated, kW; d - distance to radiometer, m; L - length of flame, m; q - heat flux at radiometer, kW/m^2; α - reflection coefficient of concrete surface below the flame.

Data from two of the ignited releases were analysed in this way, assuming a reflection coefficient for the concrete of 0.55 [4], giving an estimate of the radiative fraction as 0.054. This estimate compares reasonably well with previously reported values for gaseous and LH2 hydrogen releases [5], [6].

Using the radiative fraction above and the radiometer response during the secondary explosion, another estimate for secondary explosion size can be made. Since the explosion almost engulfed the nearest radiometers, the estimate is based on the furthest radiometer and a hemispherical heat flux. It was also assumed that the radiative fraction during the explosion was similar to that during steady burning. On this basis the quantity of hydrogen rapidly burned in the explosion was estimated as 675 g, yielding approximately 82 MJ. This would equate to approximately 18kg of TNT which is considerably higher than the upper limit suggested by the pressure effects discussed in 3.2.1. This may be attributed to the explosion yield of the hydrogen mass being less than 100%. It has been reported that hydrogen explosions with a particular energy content would cause less damage at a given distance than a mass of TNT with the same energy content [7], [8].

3.3. Overpressure Estimate

The use of Polycarbonate (4 kg TNT) in method is conservative as no windows in the shed were broken. The next closest approximation available in Hazl is annealed glass which would require 2.7 kg TNT to break. Assuming 2.7 kg of TNT as a closer approximation, this value was taken as the input condition for modelling the secondary explosion using blast program Air3D [9]. Air3D is an open source code developed to simulate three dimensional air-flows in a heterogeneous, anisotropic

zone. The predicted maximum over-pressures from the model are 16 kPa (13 m from source), 28 kPa (10 m) and 73 kPa (7 m) respectively.

4. THERMAL DOSE SAFETY DISTANCES

The level of harm caused by thermal radiation can be assessed by considering the level of radiation experienced and the period of time for which this radiation level is tolerated. This can be expressed in 'thermal dose units' (TDUs), shown in Equation 3:

$$TDU = I^{\frac{4}{3}} \times t \quad (3)$$

where *TDU* - thermal dose units; I - thermal radiation intensity, kW/m^2; t - duration for which the radiation is experienced, secs.

By taking the heat flux data from the radiometers used during testing it is possible to assess the potential thermal dose caused by an ignition of LH2. The radiometers measure radiation from the IR region and thus IR burn data have been used for comparison. Table 2 shows the thermal dose levels for several harm (burn) criteria.

Table 2. Burn severity vs. thermal dose relationship

Harm caused	IR radiation thermal dose (TDU)		
	Mean	Range	
Pain	92	86-103	[10]
Threshold – 1st degree burn	105	80-130	[11], [12]
Threshold – 2nd degree burn	290	240-350	[10], [11], [13]
Threshold – 3rd degree burn	1000	860-2600	[11]

It is of note that the burning of hydrogen releases significant quantities of ultra-violet (UV) radiation compared with hydrocarbon-based fires of a similar size. However, the dosage of UV radiation must be more than twice the IR dosage to cause similar injury levels [12]. Therefore the effects of UV radiation have been excluded and IR radiation assumed to be the dominant cause of harm. By applying the average dose levels for the different 'harm' levels (shown in Table 2) to the heat flux data measured experimentally by the radiometers, it is possible to determine the time taken to reach a given harm threshold at a given distance. This technique can be applied to infer approximate safety distances for the four ignited regimes seen during testing:

1. A steady state jet-fire during high wind speed conditions > 0.6 m/s.
2. A steady state jet-fire during low wind speed conditions < 0.6 m/s.
3. The initial deflagration or 'burn back' of the release cloud to source.
4. The secondary explosion seen after the initial deflagration has occurred.

Due to the nature of the regimes above, they can be grouped further. Both the initial deflagration and the secondary explosion are events that occur within a known, comparatively short (milliseconds) timeframe. This is in comparison with the high and low wind speed jet-fires, which can be approximated to a continuous event, which can last for longer periods (minutes). Therefore, the deflagration and explosion are reviewed separately from the jet-fires.

4.1. Jet-Fire Thermal Safety Distances

A 'no harm' criterion for jet-fires has been established at 1.6 kW/m^2 [14]. This is the heat flux level at which no discomfort will be felt regardless of exposure time. In order to find the base heat radiation level for a hydrogen jet–fire, the initial peak due to burn back was discounted until a steady state level was achieved. This steady state level was then averaged for the individual radiometers to create heat

fluxes at known distances from the flame extent (extrapolated from radiometer positions and video footage). The flame extent was equated to a 5 m long, hemi-cylindrical shape emanating from the LH2 release point.

Two tests were chosen to compare jet-fires in high and low wind conditions: Tests A and B respectively. These particular tests were chosen as they had good data sets at extremes of wind condition (Test A: 2.15 m/s; Test B: 0.59 m/s), whilst both having the same South Westerly wind direction. Fig. 8 and Fig. 9 show thermal dose against exposure time at a range of distances from the flame extent with various harm levels overlaid for high and low wind speed conditions respectively. The distances shown on the graphs represent the distances of the individual radiometers from the flame extent of the jet-fire.

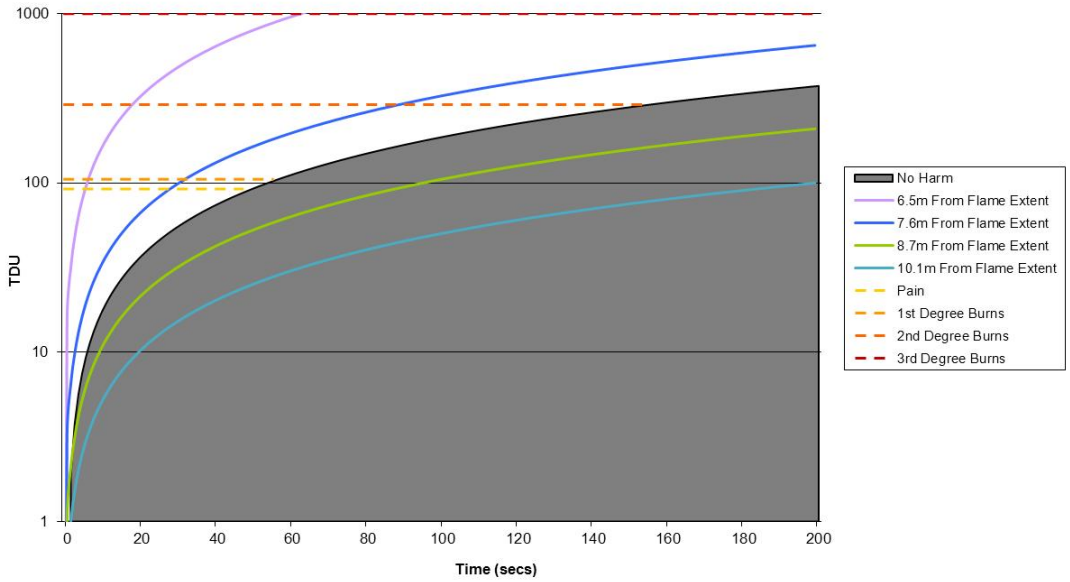

Figure 8. Thermal dose vs. exposure time during high wind conditions (Test A)

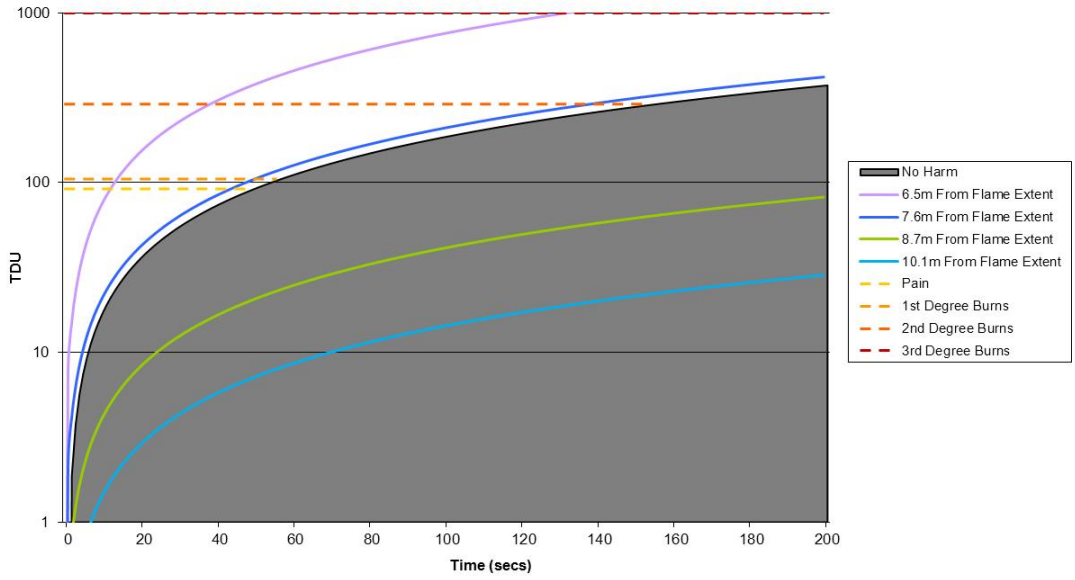

Figure 9. Thermal dose vs. exposure time during low wind conditions (Test B)

The results from these two tests indicate that at separation distances greater than 8.7m a person will not receive a harmful thermal dose regardless of exposure time. However, at distances closer than 7.6m from the flame extent, a person would expect to experience 'pain' after 28 secs and 44 seconds for high and low wind speed conditions respectively. This equates to approximately half the exposure time between a calm and windy day when closer than 7.6m from the flame extent, or 12.6m from the release point if the 5m long jet fire was directly towards you. .

4.2. Initial Deflagration/Secondary Explosion Thermal Safety Distances

The only data set that contained both an initial deflagration and then a secondary explosion was Test C. The flammable cloud extent and epicentre of the secondary explosion have been estimated from IR video footage and simplified accordingly.

The flame extent for the 'burn-back' was equated to a 9 m long, hemi-cylindrical shape emanating from the LH2 release point. From IR footage of the test, it is clear that the greatest intensity of burning occurs when the flame approaches the source at a distance of approximately 3 m (close to the secondary explosion source). Therefore, it is preferable to assume a smaller flame extent to take into account the lower intensity of flame seen at distances between 3 and 9 m.

The flame extent for the secondary explosion was equated to an 8 m diameter hemisphere emanating from a point source 2.5 m from the release point on a centreline, in line with the release.

As the initial deflagration and secondary explosion are finite and relatively short events in comparison with a continuous jet-fire, the thermal dose for these phenomena can be plotted as a function of distance from the flame extent. The assumption is made that a person would be unable to escape the event and would experience the total heat flux from the phenomena at a given distance instantly. A plot of heat flux against distance for Test C is shown in Fig. 10.

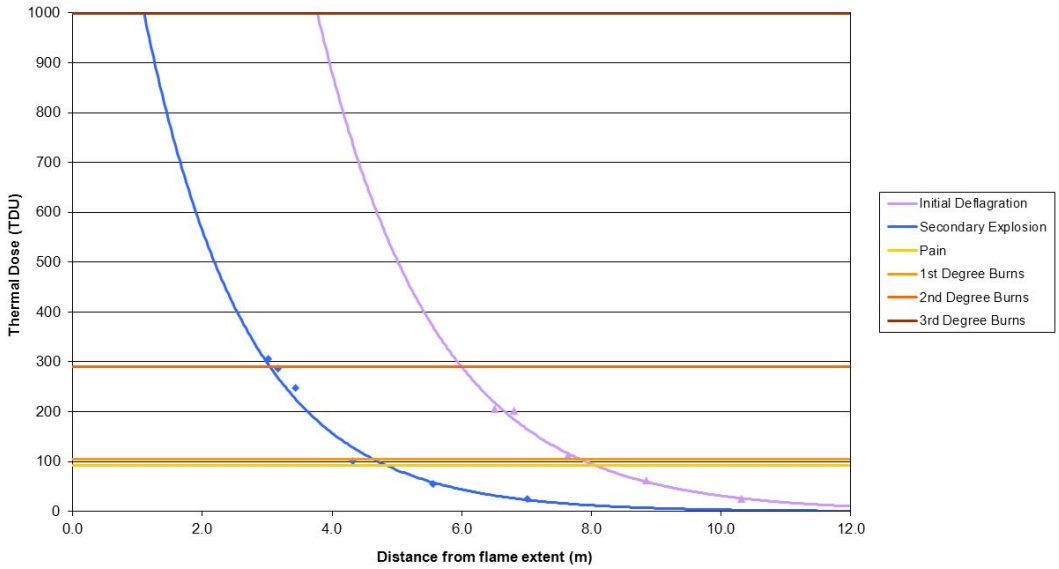

Figure 10. Thermal dose vs. distance from relevant flame extent for initial deflagration and secondary explosion (Test C).

5. CONCLUSIONS

From experimentation, four separate regimes have been found to occur when a full bore failure of a 1" liquid (60 l/min) hydrogen tanker transfer hose is ignited:

- An initial deflagration of the cloud back to source, travelling at speeds up to 50 m/s;
- A possible secondary explosion emanating from the solid deposit generated after the initial deflagration of the release cloud due to oxygen enrichment. This was estimated to have an equivalent energy of up to 4 kg of TNT;
- A buoyancy driven jet-fire when wind conditions are minimal (wind speeds < 0.6 m/s), with flame speeds > 25 m/s;
- A momentum dominated jet-fire when wind conditions are high (wind speeds > 0.6 m/s), with flame speeds > 50 m/s.

From radiometer data recorded during testing, it has been possible to estimate safety distances for the different release phenomena associated with a full bore failure of a LH2 refuelling hose (Table 3). In order to do this, different assumptions have been made for the different phenomena based on visual information from the testing and previous work on harm criteria and TDU levels. It must be pointed out that the safety distances described below are for IR radiation only and do not consider any potential pressure effects which may require greater distances. The distances represent the minimum separation distance required for an individual to stand from the release point (rupture point) to avoid feeling 'pain'. These safety distances are calculated by adding the separation distances from the flame extent (Fig. 8, 9 and 10) to the maximum flame extents for each phenomenon. This therefore describes the worst case distance from a person to an ignited LH2 hose rupture point, illustrated in Fig. 11 with the LH2 release point taken as the centre point for the separation distances.

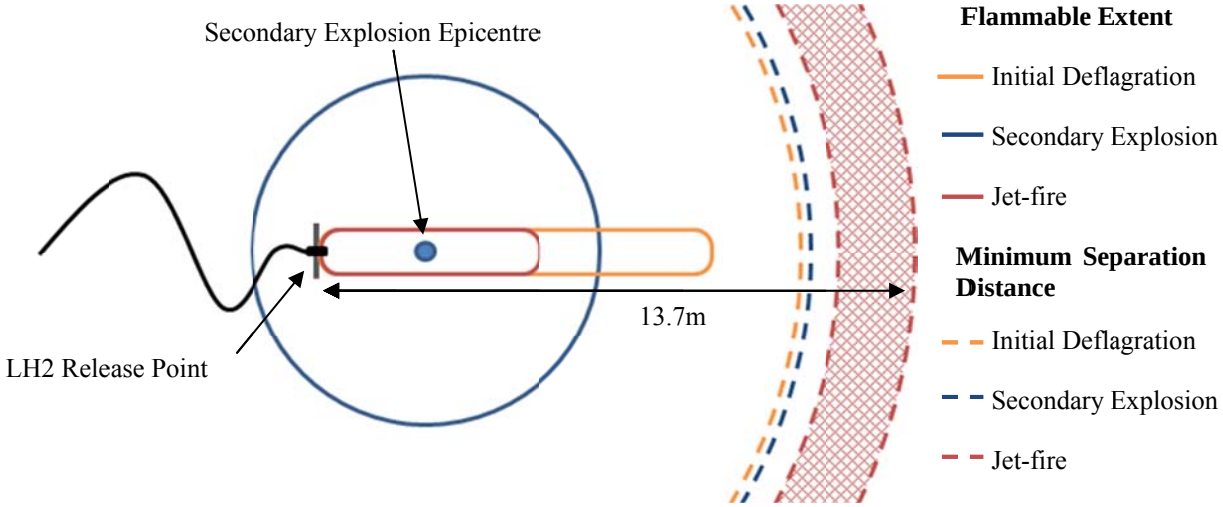

Figure 11. Scale drawing of flammable extent and minimum separation distances for the initial deflagration, secondary explosion and jet-fire.

The safety distance guide values for the four different phenomena are very similar (11 > 14m) (Table 3). This similarity in the case of the initial deflagration and secondary explosion is coincidental. Intuitively, one might expect the secondary explosion to have a larger separation distance as it has a greater peak heat flux, however, the initial deflagration is comparatively a far longer event and thus commands a greater separation distance The distances of 12.6 > 13.7 m for the jet-fires is linked to the positioning of the instrumentation but is based on exposure time at that distance. These separation distances relate to the hydrogen flow rate of 60 l/min and cannot be assumed or extrapolated for different flow rates. It is also of note that the findings and safety distance information presented in this paper are based on limited data and thus are estimates.

Table 3: Safety distance guide for thermal effects for a 60 l/min spill

	Initial cloud deflagration	Secondary explosion	Jet-fire (High wind)	Jet-fire (Low wind)
Minimum separation distance from source to avoid 'pain' (m)	> 11.1	> 11.3	12.6 > 13.7	12.6 > 13.7
Exposure time (secs)	0	0	∞	∞
Note: These values consider radiative heat only, not pressure effects				

6. REFERENCES

1. Royle, M., Willoughby, D.B., Releases of Un-ignited Liquid Hydrogen, Health and Safety Laboratory Report XS/11/70.
2. Batt, R., Webber, D. M., Modelling of Liquid Hydrogen Spills, Health and Safety Laboratory ReportMSU/2012/01.
3. Casssutt, L. H., Maddocks, F. E., and Sawyer, W. A., A Study of the Hazards in Storage and Handling of Liquid Hydrogen, Air Force Technical Data Center Doc. No. 61-05-5182.
4. McEvoy, A., Markvart, T. and Castalzer, L., Practical Handbook of Photovoltaics: Fundamentals and Applications, 2003,Academic Press; 2nd edition.
5. Studer, E. et al, Properties of Large-scale Methane/Hydrogen Jet Fires, *International Journal of Hydrogen Energy*, **34**, No. 23, 2009, pp. 9611-9619.
6. Friedrich, A. et al, Ignition and Heat Radiation of Cryogenic Hydrogen Jets, International Journal of Hydrogen Energy, **37**, No. 22, 2012, pp. 17589-17598.
7. Bodurtha, F. T., Industrial Explosion Prevention and Protection, 1980, E. I. du Pont de Nemours & Company, New York.
8. Dorofeev, S. B., Evaluation of Safety Distances Related to Unconfined Hydrogen Explosions, Proceedings of the International Conference on Hydrogen Safety, 8-10 September 2005, Pisa, No. 100129.
9. Joss, C. J. and Baehr, A. L., AIR3D, An Adaptation of the Ground-Water-Flow Code MODFLOW to Simulate Three-Dimensional Air Flow in the Unsaturated Zone, 1995, U.S. Geological Survey Open-File Report 94-533, 154 p.
10. Stoll, A.M. and Green, L.M., The production of burns by thermal radiation of medium intensity, *American Society of Mechanical Engineers*, 1958, A-219.
11. Mehta, A. K., Wong, F. and Williams, G. C., Measurement of Flammability and Burn Potential of Fabrics, Summary report to NSF-Grant #GI31881, MIT.
12. Tsao, C. K.and Perry, W. W., Modifications to the Vulnerability Model: A Simulation System for Assessing Damage from Marine Spills 9VM4, ADA 075 231, US Coast Guard NTIS Report No. CG-D-38-79.
13. Arnold et al, Hazards from Burning Garments, Gillette Research Institute, NTIS: COM -73-10957.
14. EIGA, Determination of Safety Distances, IGC Doc 75/07/E.